High-Q Wavelength Division Multiplexed Optoelectronic Oscillator based on a Cascaded Multi-loop Topology

Georgios Charalambous, G. K. M. Hasanuzzaman, Andreas Perentos, and Stavros Iezekiel[*]

Department of Electrical & Computer Engineering, University of Cyprus, Nicosia 1678, Cyprus

*Corresponding author: iezekiel@ucy.ac.cy

Abstract: A WDM optoelectronic oscillator (OEO) based on a cascaded optical multi-loop configuration and multiple photodiodes is proposed and demonstrated experimentally. By employing up to three lasers widely separated in wavelength along with two cascaded multi-loop fiber sections and two photodiodes, we demonstrate OEO topologies that scale up to six effective loops revealing an ultra-high quality factor in excess of 10^{10} and a phase noise performance down to -119 dBc/Hz at 10 kHz offset

Keywords:Optoelectronic oscillator, WDM, FIR filter, Microwave Photonics.

Introduction:

Since it was first reported in 1995, the optoelectronic oscillator has attracted much interest owing to the high quality and low phase noise microwave signals that can be generated [1]. The simplest topology consists of a single closed hybrid loop containing an optical path (typically several km of single mode fiber which acts as an energy storage element) and a microwave path (typically containing an amplifier, bandpass filter, and RF output coupler). The trade-off between high Q-factor and the presence of side modes for single-loop OEOs with long fiber lengths is well documented. This has resulted in a plethora of techniques aimed at simultaneously suppressing the side modes whilst maintaining a high Q-factor [2, 3], with optoelectronic oscillators having been demonstrated up to mm-wave frequencies [4].

A popular method for side mode suppression is based on the use of multi-loop configurations. This approach was first developed by Yao and Maleki [5], in which the optical part of the loop was split into two parallel paths – a long loop in order to establish a high Q-factor (but small FSR) and a short loop with a large FSR – which are then recombined to produce a Vernier effect. In [5], the loops were recombined coherently (after individual photodetection) via a microwave coupler. A similar strategy has been adopted in other work to show how more than two paths may be employed to optimize the phase noise reduction [6] or how multicore fibers may replace multiple fiber spools [7]. In [8] injection locking was used in conjunction with a dual

loop topology to suppress the side modes. Instead of using a classical dual loop configuration, a single loop configuration with a quality multiplier (an electronic feedback circuit designed to reduce the bandwidth of the microwave bandpass filter) has also been used filter to increase the side mode suppression ration (SMSR) [9]. In all of these approaches a single optical source is used.

It is also possible to recombine multiple loops optically through the use of multiple wavelengths, although interference effects may arise when the beams are superimposed. Other techniques for multi-loop topologies comprise multiplexing configurations where fiber Bragg grating (FBG) reflectors are used to separate the different wavelengths into different paths prior to detection in a single photodiode [10]. However, these configurations suffer from optical carrier dispersion and coherence problems due to the recombination of the optical carrier with its reflection. As a consequence, the quality factor and phase noise performance of the OEO at low offsets is degraded. In [11] a dual-wavelength dual-loop topology free from interference effects was demonstrated in conjunction with one photodiode, exhibiting a µHz class Q-factor and a phase noise of -125 dBc/Hz at a 10 kHz offset. This topology was further enhanced by the same authors through the implementation of feedback control for highly stable operation [12].

In this study, we aim to extend the above techniques by proposing and demonstrating a new approach in which the multi-loop topology of [5] is combined with the wavelength division multiplexing employed in [11]. Our topology is in essence based on a cascade of two finite impulse response (FIR) multiple source microwave photonic filters [13], in which interference beating effects are avoided because the employed wavelengths are coarsely spaced. Considering the microwave photonic filter portion of the resulting OEO, the number of taps is given by the product of the number of lasers and photodiodes used; alternatively, this product is seen to represent the number of effective loops in the overall OEO. The effect on phase noise reduction due to scaling in the number of laser sources and/or photodiodes is examined experimentally. With three lasers and two photodiodes available, we were able to implement up to six effective loops; the implemented OEO exhibits an ultra-high quality factor in excess of 10^{10} and a phase noise performance in the range -115 dBc/Hz to -125 dBc/Hz at 10 kHz offset, with this improving for an increased number of effective loops.

Proposed Architecture and Concept:

The proposed OEO concept is depicted in Fig. 1. An array of N widely and equally spaced optical carriers is combined and fed to a Mach-Zehnder Modulator (MZM). A subsequent demultiplexer (DMUX) separates the modulated optical carriers, which then traverse optical cavities implemented as single mode fibers (SMF) of lengths L_1through to L_N. The individual fibers are then recombined using a multiplexer (MUX). Previously reported WDM multiloop OEOs [10-12] are implemented using a single photodiode (PD), resulting in an effective number of loops equal to the number of optical cavities (or sources), in this instance N_S. In this scheme, we consider a second successive optical multiloop section composed of N_P different delays with

each optical section fed to a separate PD. Between the RF input to the MZM and the RF combiner output, the configuration can be regarded as a dual section FIR microwave photonic filter with a higher number of taps ($N_S N_P$) compared to using either the WDM section or multiloop section in isolation. In the context of microwave photonic FIR filters, increasing the number of taps will increase the filter's Q [14]. The WDM multiloop OEO structure is completed by connecting the RF combiner to the RF input of the MZM. Under steady-state sinusoidal oscillation conditions, the overall structure will then be a recursive system in which the Q-factor will be further enhanced due to the loop gain [14] and the presence of $N_S N_P$ different loops, thereby leading to an oscillation of a higher Q-factor and potentially better phase noise performance.
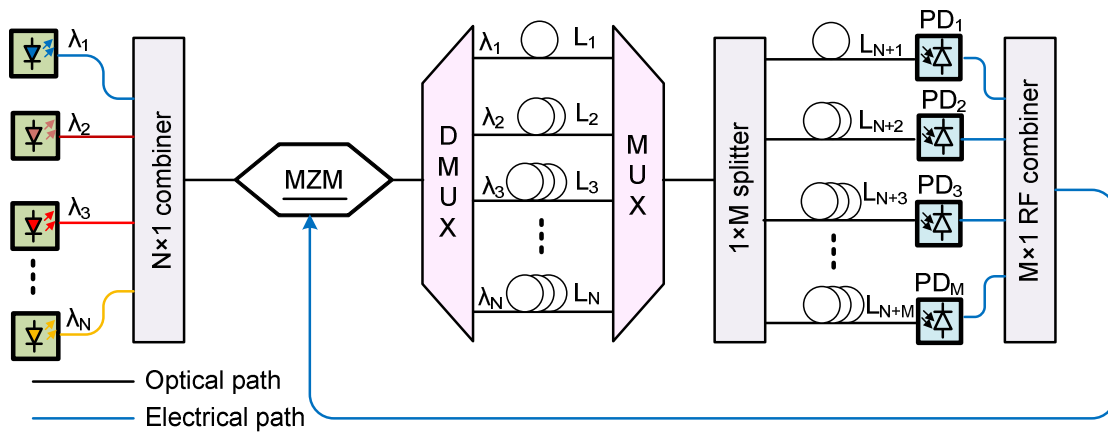

Fig. 1. Conceptual diagram of WDM multi-loop OEO. MZM: Mach-Zehnder modulator, DMUX: Demultiplexer, MUX: Multiplexer, PD: photodiode.
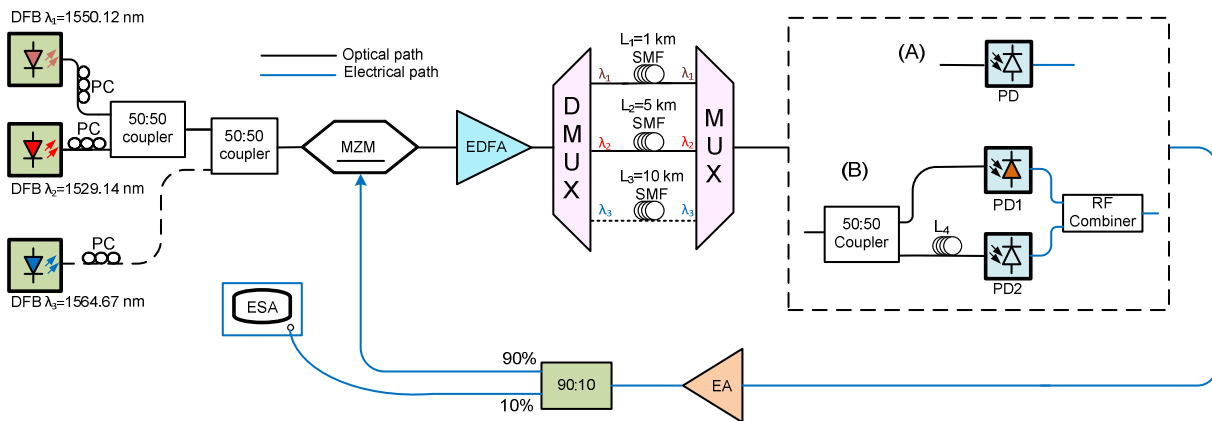

Fig. 2. Schematic diagram of the experimental WDM multi loop OEO based on either two or three laser sources and one photodiode (A) or two photodiodes (B). PC: Polarization Controller, DMUX: Demultiplexer, MUX: Multiplexer, SMF: Single Mode Fiber, ESA: Electrical Spectrum Analyzer.

Experimental Results:

The experimental setup is depicted in Fig. 2 for a system supporting up to three wavelengths ($N_S \leq 3$) and two photodiodes ($N_P \leq 2$). Systems with an effective number of loops corresponding to two ($N_P = 1$, $N_S = 2$), three ($N_P = 1$, $N_S = 3$), four ($N_P = 2$, $N_S = 2$) and six ($N_P = 2$, $N_S = 3$) were investigated. The first experiment considered an OEO with a single photodiode ($N_P = 1$, i.e. scenario (A) in Fig.2) and two independent ($N_S = 2$) continuous wave optical sources of wavelengths λ_1=1550.12 nm and λ_2=1529.14 nm of relative intensity noise (RIN) -140 dB/Hz combined with an optical coupler. The wavelength separation was sufficiently large so as to avoid beating effects in the photodiode. The two light waves fed a quadrature biased MZM with subsequent amplification via an erbium doped amplifier (EDFA) to compensate the overall optical losses. A DMUX separated the amplified light wave into two optical carriers for subsequent transmission through two different paths of fiber lengths L_1=1 km and L_2=5 km. These specific fiber lengths were chosen to suppress the intermediate side modes, as shown in Figs. 3(a) and 3(b). The two optical carriers were recombined after transmission though L_1 and L_2 via a MUX and were detected by a high speed photodiode (PD) before closing the electrical loop by connecting the PD output to the RF input of the MZM.A broadband microwave amplifier (EA) was used at the output of the PD to provide the necessary gain for sustaining a steady-state oscillation.
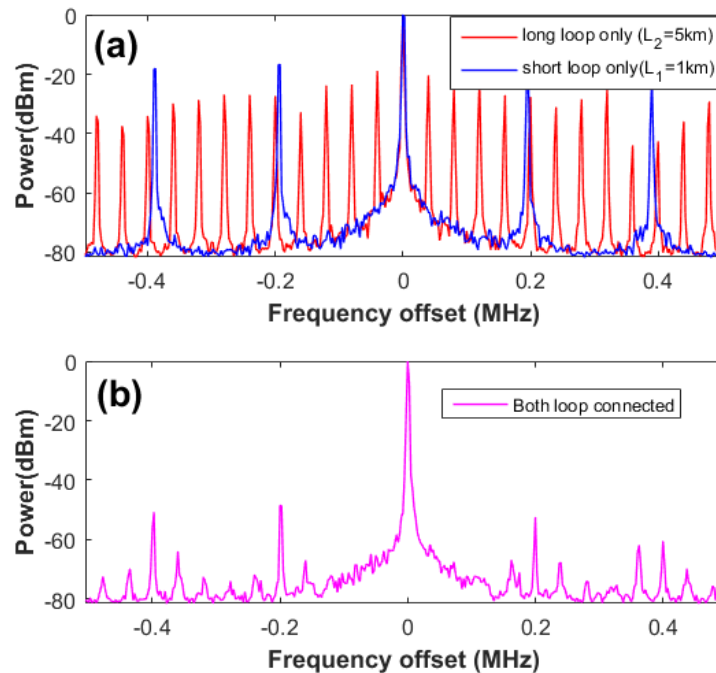

Fig. 3. Spectrum of a dual-wavelength single-photodiode (N_P= 1, N_S= 2) OEO at 1 MHz span and 1 kHz resolution bandwidth (RBW) for: (a) individual loops connected separately and (b) both loops connected. The peak oscillation is recorded at 15 GHz.

Figure 3(a) shows the measured microwave oscillation spectra of the two individual loops with the short loop (blue trace) delivering a large free spectral range (FSR) and the long loop (red trace) a narrower 3-dB bandwidth. When both loops are connected in the system, each individual loop can have a gain lower than unity but the overall loop gain of the dual-wavelength single-photodiode OEO must be greater than unity. Figure 3(b) shows the resultant microwave oscillation centered at 15 GHz obtaining its FSR from the short (1 km) loop and its 3-dB bandwidth from the long (5 km) loop. A side-mode suppression approaching 100% is observed for the long loop side modes close to the short loop central oscillating mode. Away from this central mode, exact side mode matching does not exist between the short and long loops owing to the wavelength difference between the two sources, and the suppression ratio is of the order of 30 dB.
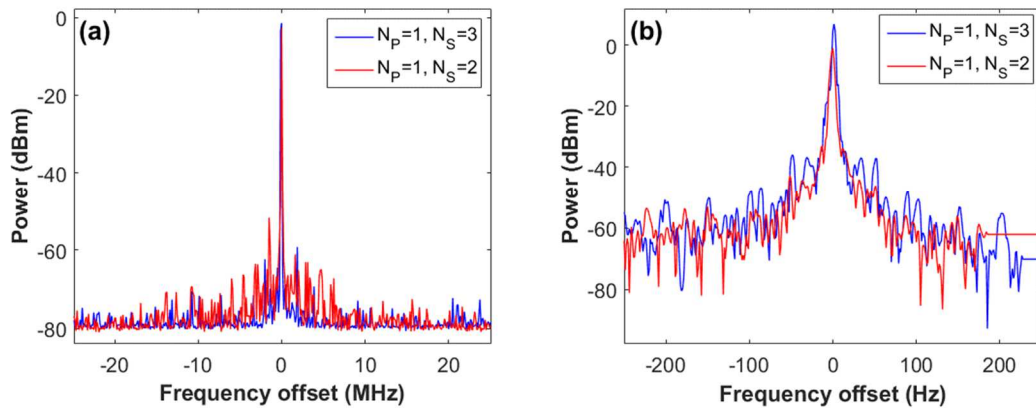

Fig. 4. Generated 15 GHz microwave oscillations for $N_S N_P$ = 2 and $N_S N_P$ = 3 effective loops at: (a) 50 MHz span and 1 kHz RBW, (b) 500 Hz span and 3 Hz RBW.

The extinction ratio (ER) of the generated oscillation is 80 dB from the peak to the noise floor and about 50 dB from the peak to the first-order side mode. The experimental setup of Fig.2was then modified to accommodate a third optical source (N_S=3) of wavelength λ_3=1564.67 nm and an extra SMF delay L_3=10 km whilst retaining a single photodiode (N_P= 1) in order to extend the number of effective loops to $N_S N_P$= 3 and thus further improve the Q-factor and the phase noise performance of the OEO. The measured 15 GHz oscillation is compared with the $N_S N_P$= 2 case in Figs. 4(a) and 4(b);the Q-factor was expected to increase with the inclusion of the 10 km SMF, but due to the RBW limit of our spectrum analyzer it was not possible to see this improvement. We therefore proceeded to measure the single side band (SSB) phase noise for the dual wavelength – single photodiode and triple wavelength – single photodiode cases to confirm any possible performance enhancement. The results are shown in Fig. 5.For the purposes of comparison, a classical dual-loop OEO topology (as in [5]) based on a single wavelength at $\lambda_1$and two fiber delays (L_1=1 km and L_2=5 km) was also implemented, in which the MUX and DMUX were substituted with 3-dB optical couplers. The phase noise of the oscillation shown in Fig. 4 was measured using the direct spectrum technique on an Agilent E4407B electrical spectrum analyzer. Note that this method cannot measure accurately very

low phase noise levels (< -101 dBc/Hz) at low frequency offsets (<10 kHz).In fact, results obtained through this technique are the combination of three different noise sources; namely the noise of the input signal, the internal noise of the analyzer (triggered by the input signal) and the displayed average noise level of the Analyzer (DANL) [15]. The DANL, an inherent phase noise source, is included in the measurement regardless of the signal being present or not and limits the range over which the analyzer can measure phase noise. To improve the accuracy of our measurements, we used the cancellation method of the analyzer's phase noise personality (option 226) which removes the effect of the analyzer's internal noise [15, 16]. This is done by comparing a stored reference measurement with the measured phase noise of the device under test. The phase noise of this single-source dual-loop OEO was measured at -100 dBc/Hz at 10 kHz offset. The setup of Fig. 2 was then implemented for the proposed topology for the cases of two effective loops ($M = 1$, $N = 2$) and three effective loops ($M = 1$, $N = 3$), yielding measured phase noise at 10 kHz offset of -108 dBc/Hz and -118 dBc/Hz respectively. Hence compared to the classical dual-loop approach of [5], using two and three effective loops reduces the phase noise by 8 dB and 18 dB respectively, indicating the potential improvement from increasing the number of effective loops.
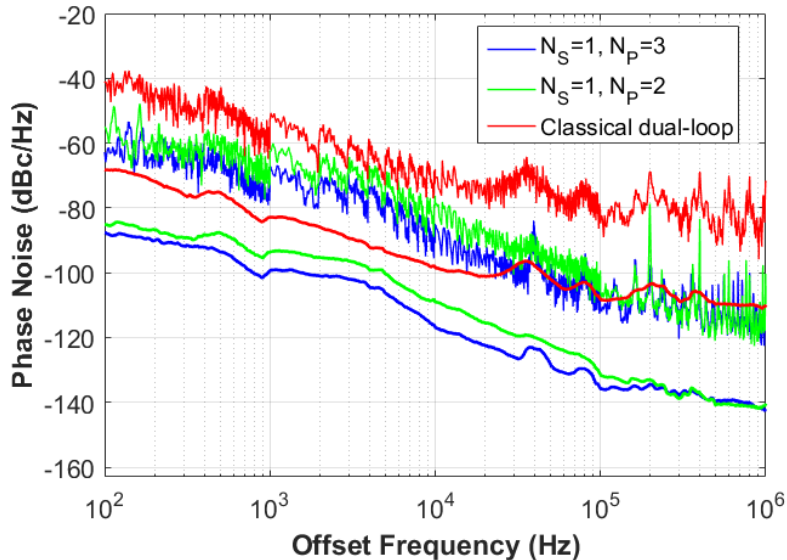

Fig. 5. Phase noise measurement comparison between the three and two optical source topology and the classical single-source dual-loop OEO. The upper set of curves was taken before applying the cancellation method on the ESA in order to observe more clearly any side mode effects at the higher offsets.

The effect of scaling the number of photodiodes was then examined by adding a second PD and an associated SMF cavity L_4 using the arrangement in section (B) of Fig.2. This topology is free from interference effects because the multiplexed inputs of PD1 and PD2 are delayed by a time equivalent to length L_4 that exceeds the coherence time of the sources. (Owing to the limited number of fiber spools available, $L_4 =10$ km for the $N_S N_P = 4$ loops case and 20 km for the $N_S N_P = 6$ loops case.)The main oscillation was generated at 5.5 GHz for four effective loops ($N_P = 2$, $N_S =$

2) and 5.6 GHz for six effective loops (N_P = 2, N_S = 3) as shown in Figs 6(a)-6(d). When the number of effective loops is increased from two to four, a dramatic improvement in the extinction ratio of the oscillation with respect to the first-order side mode is achieved, it increasing from 50 dB to 70 dB. The 3-dB bandwidth is also expected to be narrower although the net improvement could not be measured due to the RBW limit of the ESA that was used. In the scenario where the 3-loop (N_P= 1, N_S = 3) topology is increased to 6 loops (N_P = 2, N_S = 3), no noticeable spectral improvement is recorded; this is attributed to the noise floor limit of the ESA. The phase noise performance was measured in the same way as described for Fig. 5 and results are shown in Fig.7.
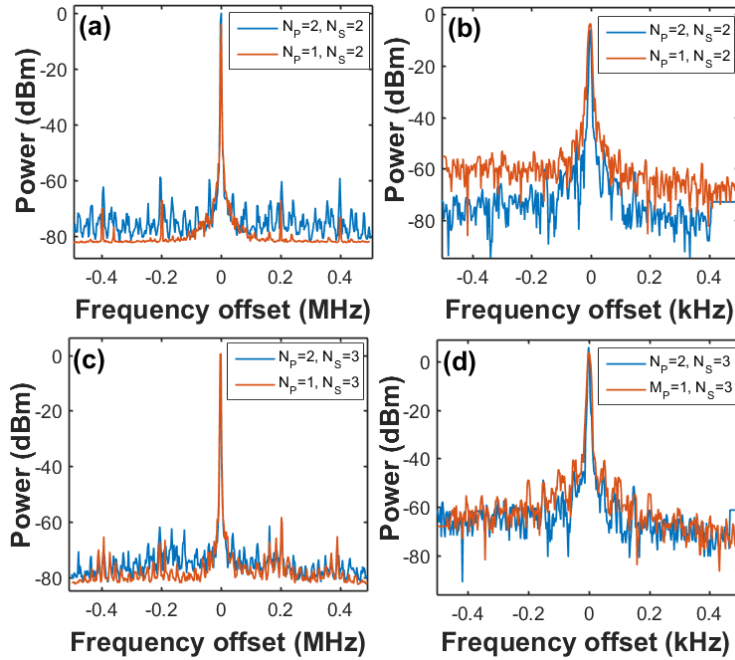

Fig. 6. Electrical spectra of the generated microwave oscillations using one PD and two PDs with two optical sources at: (a) 1 MHz span and1 kHz RBW, (b) 1 kHz span and 3 Hz RBW, and with three optical sources at: (c) 1 MHz span and 1 kHz RBW and (d) 1 kHz span and 3 Hz RBW.

At 10 kHz offset and for the (N_P= 2, N_S= 2) scenario, i.e. four effective loops, a phase noise of -116 dBc/Hz is recorded as shown in Fig. 7(a), thus outperforming the (N_P= 1, N_S= 2) system by 8 dB. For the triple-wavelength dual-PD scenario, i.e. six effective loops, a phase noise of -119 dBc/Hz is recorded as shown in Fig. 7(a), thereby not showing any significant improvement in comparison to the (N_P= 1, N_S= 3) system. This is attributed to a limitation of the employed ESA (Agilent E4407B) which cannot distinguish phase noise levels when operating near the noise floor of the instrument.
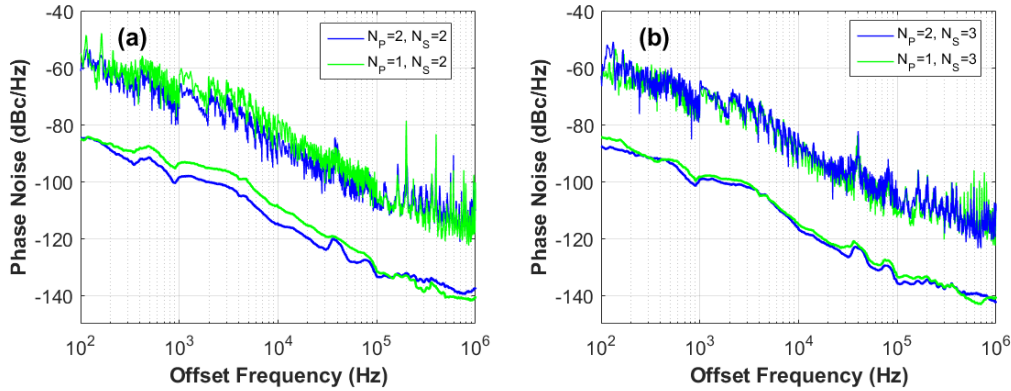
Fig. 7. Single side-band (SSB) phase noise measurements for (a) dual-wavelength topology and (b) triple-wavelength topology as a function of the number of photodiodes. The upper set of curves was taken before applying the cancellation method on the ESA in order to observe more clearly any side mode effects at the higher offsets.

OEOs based on standard single mode silica optical fibers exhibit length and refractive index variations of the order of 0.1 ppm/^{o}C and 10 ppm/^{o}C respectively due to temperature changes. Consequently, the frequency instability of the generated microwave signal is of the order of 10 ppm/^{o}C. In contrast, replacing SMF-28 fibers with photonic crystal fibers (PCF) reduces the frequency and index variations, while a decrease of the thermal sensitivity by a factor of three can be achieved (but at the expense of degraded phase noise performance) [17]. The temperature dependence can also be minimized by controlling the temperature variations of the Q-elements by using a control circuit and resistive heaters or packaging the OEO by integrating the optical and microwave devices into a circuit board. Another source of instability is the variation of the MZM's bias point due to temperature variations, coupling efficiency and photo-refractive effects. Bias control systems can be implemented to detect and correct the modulator bias drifts in order to improve the frequency stability of the OEO [18]. The frequency stability can also be improved through nonlinear electronic feedback techniques [19].

For a single optical source OEO, the contribution of laser low frequency RIN (power noise) to microwave phase noise has been shown to be minor [20]. It is shown in the same study that wavelength fluctuations (frequency noise) is the dominant contributor to phase noise through the chromatic dispersion that is introduced from the long optical fiber delay line. In our system, we employ three free-running and coarsely separated (20 nm spacing) DFB lasers, each with an identical RIN specification of -140 dB/Hz. Taking into account the low RIN for each laser, we believe that optical frequency noise will have a more severe impact on the microwave phase noise than the total power noise (RIN) of the system [20]. This can be mitigated by replacing the standard single mode fiber sections with zero dispersion fiber delay lines. Although the RIN contribution is not as significant, it can be reduced if the received optical power saturates the photodiodes [21] and also through the use of a saturated semiconductor optical amplifier [21]. Finally, replacing individual sources with a stable low-RIN optical comb may further improve the OEO phase noise performance.

The measured characteristics of the four OEOs that were implemented are compared in Table 1.This shows that increasing either the number of optical wavelengths or photodiodes in the topology will yield an improved phase noise performance and an increase on the ratio between the center oscillation frequency and the first-order side mode. In this work we elected not to include a microwave bandpass filter in the loop, thus the oscillation frequencies were determined by the cascaded FIR sections which explains the change in oscillation frequency for the different cases in table 1.

		N_P=1	N_P=2
	N_S=2	PN=-108dBc @ 10 kHz Side Mode Ratio=50 dB CF= 15 GHz	PN=-116dBc @ 10 kHz Side Mode Ratio = 60 dB CF =5.5 GHz
	N_S=3	PN=-118dBc @10kHz Side Mode Ratio = 60 dB CF = 15 GHz	PN=-119dBc @ 10 kHz Side Mode Ratio = 70 dB CF = 5.6 GHz

Table 1. Comparison of the experimental performance for different numbers of optical sources (N_S) and photodiodes (N_P). PN = phase noise, CF = center frequency of oscillation.

Conclusion:

In conclusion, we have demonstrated an OEO topology based on the cascade of a WDM FIR section with a multiloop FIR section which results in a number of effective loops given by the product of the number of sources and number of photodiodes used. We have examined the impact of increasing the number of effective loops and shown that it is possible to achieve a Q-factor in excess of 10^{10} with a phase noise approaching -120 dBc/Hz at 10 kHz offset. In principle the topology can be scaled to a larger number of effective loops. This would necessitate an alternative implementation in order to reduce the component count. For example, a multiple wavelength source such as a mode locked laser or a travelling wave photodiode array [22] could be used to minimize the number of discrete component.

Acknowledgement:

References:

[1] S. Iezekiel, Microwave Photonics: Devices and Applications, Wiley, 2009.

[2] X. Yao and L. Maleki, Optoelectronic microwave oscillator, J. Opt. Soc. Am. B. 13 (1996)1725.

[3] G. Charalambous, A. Perentos and S. Iezekiel, High- Q Optoelectronic Oscillator Based on Active Recirculating Delay Line and Dual-Loop Topology, IEEE Photon. Technol. Lett.28 (2016) 2850-2853.

[4] S. Fedderwitz, A. Stöhr, S. Babiel, V. Rymanov and Dieter Jäger, Opto-electronic dual-loop 50 GHz oscillator with wide tunability and low phase noise, 2010 IEEE Topical Meeting on Microwave Photonics (MWP), pp. 224-226, 2010.

[5] X. Yao and L. Maleki, Multiloop optoelectronic oscillator, IEEE J. Quantum Electron. 36, (2000) 79-84.

[6] T. Bánky, B. Horváth and T. Berceli, Optimum configuration of multiloop optoelectronic oscillators, J. Opt. Soc. Am. B 23, (2006), 1371.

[7] S. García and I. Gasulla, Multi-cavity optoelectronic oscillators using multicore fibers, Opt. Express 23, (2015) 2403.

[8] W. Zhou and G. Blasche, Injection-locked dual opto-electronic oscillatorwith ultra-low phase noise and ultra-low spurious level, IEEE Trans. Microw. Theory Technol. 53 (2005) 929–933.

[9] L. Bogataj, M. Vidmar and B. Batagelj, Opto-Electronic Oscillator With Quality Multiplier, IEEE Trans. Microw. Theory Technol. 64(2016) 663-668.

[10] E. Shumakher and G. Eisenstein, A Novel Multiloop Optoelectronic Oscillator, IEEE Photon. Technol. Lett. 20 (2008) 1881-1883.

[11] S. Jia, J. Yu, J. Wang, W. Wang, Q. Wu, G. Huang and E. Yang, A Novel Optoelectronic Oscillator Based on Wavelength Multiplexing, IEEE Photon. Technol. Lett. 27 (2015) 213-216.

[12] S. Jia et al., A Novel Highly Stable Dual-Wavelength Short Optical Pulse Source Based on a Dual-Loop Optoelectronic Oscillator With Two Wavelengths, IEEE Photon. J. 7(2015) 1-11.

[13] J. Capmany, B. Ortega and D. Pastor, A tutorial on microwave photonic filters, J. Lightwave Technol. 24 (2006) 201-229.

[14] L. Zhou, X. Zhang and E. Xu, Q value analysis of microwave photonic filters, Front. Optoelectron. China 2 (2009) 269-278.

[15] Literature.Cdn.Keysight.Com. (2016). http://literature.cdn.keysight.com/litweb/pdf/E4440-90233.pdf?id=1294529 (accessed 20 October 2016).

[16] http://literature.cdn.keysight.com/litweb/pdf/5988-4348EN.pdf (accessed 20 October 2016).

[17] M. Kaba et al., Improving thermal stability of opto-electronic oscillators, IEEE Microw. Magazine. (2006)38-47.

[18] D. T. Bui, T. T. Pham, V. Y. Vu and B. Journet, Improving Opto-Electronic Oscillator stability by controlling the Electro-Optic Modulator, 2012 Fourth International Conference on Communications and Electronics (ICCE), Hue, 2012, pp. 63-68.

[19] T. Banky, T. Berceli and B. Horvath, Improving the frequency stability and phase noise of opto-electronic oscillators by harmonic feedback, 2004 IEEE MTT-S International Microwave Symposium Digest (IEEE Cat. No.04CH37535), 2004, pp. 291-294 Vol.1.

[20] K. Volyanskiy, Y. K. Chembo, L. Larger and E. Rubiola, Contribution of Laser Frequency and Power Fluctuations to the Microwave Phase Noise of Optoelectronic Oscillators, J. Lightwave. Technol. 28(2010) 2730-2735.

[21] D. Eliyahu, D. Seidel and L. Maleki, RF Amplitude and Phase-Noise Reduction of an Optical Link and an Opto-Electronic Oscillator, IEEE Trans. Microw. Theory Technol. 56(2008) 449-456.

[22] S. Murthy, T. Jung, Tai Chau, M. Wu, D. Sivco, A. Cho, A novel monolithic distributed traveling-wave photodetector with parallel optical feed, IEEE Photon. Technol. Lett. 12 (2000) 681-683.